

Multidecadal Co-variability of North Atlantic Sea Surface Temperature, African dust, and Sahel Rainfall

Chunzai Wang¹

Shenfu Dong^{1 & 2}

Amato T. Evan³

Gregory R. Foltz¹

Sang-Ki Lee^{1 & 2}

¹ NOAA Atlantic Oceanographic and Meteorological Laboratory
Miami, Florida

² Cooperative Institute for Marine and Atmospheric Studies
University of Miami
Miami, Florida

³ Department of Environmental Sciences
University of Virginia
Charlottesville, Virginia

Submitted to *Nature* as a Letter

March 31, 2011

Corresponding author address: Dr. Chunzai Wang, NOAA/Atlantic Oceanographic and Meteorological Laboratory, 4301 Rickenbacker Causeway, Miami, FL 33149, USA.
E-mail: Chunzai.Wang@noaa.gov; Phone: 305-361-4325; Fax: 305-361-4412.

Previous studies regarding African dust and North Atlantic climate have been limited to a short period since the satellite era (1980 onward)^{1,2}. Here we use new datasets with records extending back to the 1950s to show a multidecadal co-variability of sea surface temperature (SST) and aerosols in the North Atlantic, and rainfall in the Sahel. When the North Atlantic Ocean was cold from the late 1960s to the early 1990s, the Sahel received less rainfall and the tropical North Atlantic experienced high concentrations of dust. The opposite was true when the North Atlantic Ocean was warm before the late 1960s and after the early 1990s. This suggests that a positive feedback exists between North Atlantic SST, African dust, and Sahel rainfall on multidecadal timescales. That is, a warm (cold) North Atlantic Ocean produces a wet (dry) condition in the Sahel and thus leads to low (high) concentration of dust in the tropical North Atlantic which in turn warms (cools) the North Atlantic Ocean. An implication of this study is that coupled climate models need to be able to simulate this aerosols-related feedback in order to correctly simulate climate variability and change in the North Atlantic.

Sea surface temperature (SST) in the North Atlantic Ocean varies mainly on two timescales: a secular warming and a multidecadal variation. There is a debate on the relative roles of anthropogenic global warming and natural climate variability in the North Atlantic SST variability³⁻⁹. In this paper, we mainly focus on the component induced by natural variability – the Atlantic multidecadal oscillation (AMO) – a climate mode occurring in the North Atlantic SST that operates primarily on multidecadal timescales^{5,10}. Here the AMO index is defined as the detrended North Atlantic SST anomalies over the region of 0°-60°N and from the east coast of the Americas to 0° longitude (Fig. 1a). The extended reconstructed SST data from 1950 to

2008 show that the AMO was in the cold phase from the late 1960s to the early 1990s and in the warm phases before the late 1960s and after the early 1990s.

The AMO has footprints on many parts of the global oceans (Fig. 1b). In addition to the basin-wide warming of the North Atlantic Ocean, the warm phase of the AMO is associated with warming in the western North and South Pacific Oceans and the tropical eastern Indian Oceans and cooling over the global Southern Oceans and in the subtropical northeastern Pacific Ocean. Opposite-signed SST anomalies occur for the cold phase of the AMO. The Atlantic SST regression shows a bipolar seesaw pattern or an inter-hemispheric gradient¹¹, supporting the hypothesis that the driving mechanism of the AMO involves fluctuations of the Atlantic meridional overturning circulation (AMOC)^{7,10}. As the AMOC is enhanced, a warming and a cooling will occur in the North and South Atlantic Oceans, respectively, and *vice versa* for a reduction of the AMOC.

AMO variability is associated with changes of climate and extreme events such as drought, flood and hurricane activity^{5,6,12-14}. Recent studies show that only the tropical portion of the AMO is relevant to climate since the climate response to the North Atlantic SST anomalies is primarily forced at the low latitudes¹⁵. Accordingly, the influence of the AMO on climate and hurricane activity may operate through the mechanism of the atmospheric changes induced by the tropical North Atlantic and Caribbean Sea¹⁶. It is therefore important to understand the mechanisms that drive multidecadal variability in the tropical North Atlantic SST.

Atlantic SST and its inter-hemispheric gradient have been recognized to relate to and to force drought after the 1970s in the Sahel, a region in Africa between the Saharan desert and the rainforests of Central Africa and the Guinean Coast^{17,18}. The Sahel rainfall anomalies co-vary with the AMO on multidecadal timescales (Figs. 2a and b). The warm (cold) phases of the AMO

are associated with positive (negative) rainfall anomalies in the Sahel. This relationship still holds if the AMO and Sahel rainfall time series are extended for the entire 20th century (Fig. S1). More interestingly, the dust aerosol optical depth (DAOD) in the tropical North Atlantic (described in Supplementary Information), which is proportional to mass concentration and is a proxy for atmospheric dust content, is also in phase with the AMO and the Sahel rainfall anomalies (Fig. 2c). Since the DAOD time series is highly correlated with the dust time series observed in Barbados¹⁹ and the DAOD data is longer than the station data in Barbados, we use the DAOD data to study multidecadal variation in this paper.

When the North Atlantic Ocean was cold during the late 1960s to the early 1990s, the Sahel received less rainfall and the tropical North Atlantic had high concentrations of dust. The opposite was true for the warm phases of the AMO after the early 1990s and before the late 1960s. We smooth each time series with a 7-year running mean filter and calculate the correlations among these filtered indices. The correlations of the AMO index with the Sahel rainfall and DAOD anomalies are 0.81 and -0.67, respectively, and the correlation between the Sahel rainfall and DAOD anomalies is -0.85. All of these correlations are statistically significant based on student's t-test (above 99% significant levels).

To emphasize AMO-related variability, we have detrended all data (i.e., removed linear trends). We also plot the data with the linear trends included; that is, data that includes the components of global warming and the AMO (Figs. S2 and S3). A comparison of Fig. 1b and Fig. S2b indicates that the global warming signal is spread throughout most of the global oceans. With the global warming trend included, the rainfall anomalies in the Sahel show negative anomalies during the warm phase of the AMO after the early 1990s (Fig. S3b). This indicates that the impacts of global warming and the AMO on rainfall in the Sahel are opposite in sign.

The DAOD anomalies in Fig. S3c are almost identical to those in Fig. 2c, indicating that the DAOD data used here do not have a significant long-term linear trend.

The spatial rainfall patterns related to the AMO and aerosols in the tropical North Atlantic are shown in Fig. 3. A strong positive AMO-rainfall regression stands out in the Sahel region (Fig. 3a). This indicates that on multidecadal timescales the warm (cold) North Atlantic Ocean corresponds to more (less) rainfall in the Sahel. The positive AMO phase leads to a northward shift of the intertropical convergence zone (ITCZ)^{20,21}. Since the northward shift of the Atlantic ITCZ is associated with the anomalous moisture convergence in the lower troposphere and upward motion at 500-hPa (Fig. 3c) over the Sahel, Sahel rainfall is enhanced. Figure 3a also shows the significant rainfall patterns associated with the AMO from North America to equatorial South America, consistent with previous studies^{5,6}. The dust-rainfall regression shows that high (low) concentration of dust in the tropical North Atlantic is associated with less (more) rainfall in the Sahel on multidecadal timescales (Fig. 3b). For the data with the global warming trend included, the positive AMO-rainfall regression in the Sahel region is largely reduced (Fig. S4) due to the offsetting effect of global warming. Our analyses here suggest that global warming decreases rainfall in the Sahel, whereas the warm phase of the AMO after the early 1990s increases rainfall in the Sahel.

Previous studies have shown that Atlantic dust storm frequency and intensity changes are forced by variability in Sahelian precipitation²². The question is: What is the mechanism for the negative relationship between Sahel rainfall and dust in the tropical North Atlantic on multidecadal timescales? One possibility is that anomalously high precipitation causes a “greening” of the Sahel²³ and thus shrinking of dust source regions, increase in soil moisture, and decrease in surface shear stress acting on soils where vegetation is present²⁴. It is also possible

that surface winds play an important role. The composite wind map shows increased surface wind speed across the Sahel and the southern sector of the Sahara (Fig. 4) during periods of high DAOD in the tropical North Atlantic. An increase in surface wind speed over dust source regions such as the Bodéle Depression²⁵ would lead to increased atmospheric dust loading since deflation is proportional to surface shear stress²⁴. The enhanced surface winds in western Africa are associated with a weakening of the southwesterly monsoon flow, which in turn is connected to the observed decrease in Sahel precipitation¹⁸.

The wind composite also shows strong surface easterly wind anomalies in the tropical region (Fig. 4), which would tend to enhance dust transport over the Atlantic Ocean. However, transport of Saharan dust westward from the African coast is most strongly correlated with winds at about 700-hPa²⁶. The regressed winds at 700-hPa and 850-hPa show that the maximum easterly wind anomalies are south of the maximum dust band between 10°-20°N (Fig. S5). The inconsistency suggests that the dust changes in the tropical North Atlantic could be more due to enhanced dust production in the Sahel and Saharan regions, as evidenced by the increase in precipitation and surface wind over these source regions. If more dust production occurs over the Sahel and Saharan regions, then the tropical North Atlantic will experience higher dust concentrations because of transport by the mean easterly trade wind. Changes in dustiness in the tropical North Atlantic in turn force a significant portion of the underlying SST variability on interannual to decadal timescales by changing the amount of solar radiation reaching the ocean's surface^{1,27}.

The observed results suggest that a feedback process between the AMO and dust in the tropical North Atlantic may operate through Sahel rainfall variability. Suppose an initial warm North Atlantic. The warm North Atlantic is associated with a northward shift of the Atlantic

ITCZ and southwesterly wind anomalies, and thus results in an increase of rainfall in the Sahel. The increased rainfall leads to an increase in vegetation across the Sahel²³ and a decrease in source regions for mineral aerosols²⁸. Associated with the decrease of aerosols in arid regions of Africa is a decrease of atmospheric wind-blown dust over the tropical North Atlantic. The decrease of dust in the tropical North Atlantic, in turn, is a positive feedback onto tropical North Atlantic SST via the aerosol direct effect^{1,27}. However, further studies are needed to quantify the impact of dust forcing on North Atlantic SST and to determine the processes controlling African dust emission on multidecadal timescales.

Almost all coupled climate models have difficulty in simulating the magnitude of the AMO²⁹, and the reason may be due to the lack of the positive dust-AMO feedback proposed here. For example, the few model experiments included in the Coupled Model Intercomparison Project (CMIP) phase 3 database that include dust, dust concentration is prescribed and does not vary from one year to the next. Furthermore, model dust concentrations are strongly dependent upon the global surface area over which deflation occurs, and there is considerable model spread in global desert area in the future warming scenarios²⁸. We thus propose that one way to examine the effectiveness of coupled models in the next CMIP database, of which many will include interactive dust, is to identify the extent to which the connection between AMO-like variability and Atlantic dust cover, as observed here, is reproduced in 20th Century experiments. Coupled climate models need to capture the aerosols-related feedback for a realistic climate simulation in the Atlantic.

References

1. Evan, A. T., et al. The role of aerosols in the evolution of tropical North Atlantic Ocean temperature anomalies. *Science* **324**, 778-781, doi:10.1126/Science.1167404 (2009).
2. Foltz, G. R. & McPhaden, M. J. Trends in Saharan dust and tropical Atlantic climate during 1980 – 2006. *Geophys. Res. Lett.* **35**, L20706, doi:10.1029/2008GL035042 (2008).
3. Trenberth, K. E. & Shea, D. J. Atlantic hurricanes and natural variability in 2005. *Geophys. Res. Lett.* **33**, L12704, doi:10.1029/2006GL026894 (2006).
4. Mann, M. E. & Emanuel, K. A. Atlantic hurricane trends linked to climate change. *Eos Trans. AGU* **87**, 233-244, doi:10.1029/2006EO240001 (2006).
5. Enfield, D. B., Mestas-Nunez, A. M. & Trimble, P. J. The Atlantic Multidecadal Oscillation and its relationship to rainfall and river flows in the continental US. *Geophys. Res. Lett.* **28**, 2077-2080 (2001).
6. McCabe, G., Palecki, M. & Betancourt, J. Pacific and Atlantic Ocean influences on multidecadal drought frequency in the United States. *Proc. Nat. Acad. Sci.* **101**, 4136-4141 (2004).
7. Knight, J. R., Allan, R. J., Folland, C. K., Vellinga, M. & Mann, M. E. A signature of persistent natural thermohaline circulation cycles in observed climate. *Geophys. Res. Lett.* **32**, L20708, doi:10.1029/2005GL024233 (2005).
8. Zhang, R., Delworth, T. L. & Held, I. Can the Atlantic Ocean drive the observed multidecadal variability in Northern Hemisphere mean temperature? *Geophys. Res. Lett.* **34**, L02709, doi:10.1029/2006GL028683 (2007).

9. Wang, C. & Dong, S. Is the basin-wide warming in the North Atlantic Ocean related to atmospheric carbon dioxide and global warming? *Geophys. Res. Lett.* **37**, L08707, doi:10.1029/2010GL042743 (2010).
10. Delworth, T. L. & Mann, M. E. Observed and simulated multidecadal variability in the Northern Hemisphere. *Clim. Dyn.* **16**, 661-676 (2000).
11. Stocker, T. F. The seesaw effect. *Science* **282**, 61-62 (1998).
12. Goldenberg, S. B., Landsea, C., Mestas-Nunez, A. M. & Gray, W. M. The recent increase in Atlantic hurricane activity. *Science* **293**, 474-479 (2001).
13. Bell, G. D. & Chelliah, M. Leading tropical modes associated with interannual and multidecadal fluctuations in North Atlantic hurricane activity. *J. Clim.* **19**, 590-612 (2006).
14. Wang, C. & Lee, S.-K. Co-variability of tropical cyclones in the North Atlantic and the eastern North Pacific. *Geophys. Res. Lett.* **36**, L24702, doi:10.1029/2009GL041469 (2009).
15. Sutton, R. T. & Hodson, D. L. R. Climate response to basin-scale warming and cooling of the North Atlantic Ocean. *J. Clim.* **20**, 891-907 (2007).
16. Wang, C., Lee, S.-K. & Enfield, D. B. Atlantic warm pool acting as a link between Atlantic multidecadal oscillation and Atlantic tropical cyclone activity. *Geochem. Geophys. Geosyst.* **9**, Q05V03, doi:10.1029/2007GC001809 (2008).
17. Folland, C. K., Palmer, T. N. & Parker, D. E. Sahel rainfall and worldwide sea temperatures, 1901-85. *Nature* **320**, 602-607 (1986).
18. Giannini, A., Saravanan, R. & Change, P. Oceanic forcing of Sahel rainfall on interannual to interdecadal time scales. *Science* **302**, 1027-1030 (2003).

19. Evan, A. T. & Mukhopadhyay, S. African Dust over the Northern Tropical Atlantic: 1955–2008. *J. Appl. Meteor. Climatol.*, **49**, 2213–2229 (2010).
20. Zhang, R. & Delworth, T. L. Impact of Atlantic multidecadal oscillations on India/Sahel rainfall and Atlantic hurricanes. *Geophys. Res. Lett.* **33**, L17712, doi:10.1029/2006GL026267 (2006).
21. Krebs, U. & Timmermann, A. Tropical air-sea interactions accelerate the recovery of the Atlantic Meridional Overturning Circulation after a major shutdown. *J. Clim.* **20**, 4940–4956 (2007).
22. Prospero, J. M. & Lamb, P. J. African droughts and dust transport to the Caribbean: Climate change implications. *Science* **302**, 1024–1027 (2003).
23. Nicholson, S. E., Tucker, C. J. & Ba, M. B. Desertification, drought, and surface vegetation: An example from the West African Sahel. *Bull. Amer. Meteor. Soc.* **79**, 815–829 (1998).
24. Marticorena, B., et al. Modeling the atmospheric dust cycle: 2. Simulation of Saharan dust sources. *J. Geophys. Res.* **102**, 4387–4404 (1997).
25. Washington, R., et al. Links between topography, wind, deflation, lakes and dust: The case of the Bodélé Depression, Chad. *Geophys. Res. Lett.* **33**, L09401, doi:10.1029/2006GL025827 (2006).
26. Kaufman, Y. J., et al. Dust transport and deposition observed from the Terra-Moderate Resolution Imaging Spectroradiometer (MODIS) spacecraft over the Atlantic Ocean. *J. Geophys. Res.* **110**, D10S12, doi:10.1029/2003JD004436 (2005).
27. Foltz, G. R. & McPhaden, M. J. Impact of Saharan dust on tropical North Atlantic SST. *J. Clim.* **21**, 5048–5060 (2008).

28. Mahowald, N. M. Anthropocene changes in desert area: Sensitivity to climate model predictions. *Geophys. Res. Lett.* **34**, L18817, doi:10.1029/2007GL030472 (2007).
29. Knight, J. R. The Atlantic multidecadal oscillation inferred from the forced climate response in coupled general circulation models. *J. Clim.* **22**, 1610-1625 (2009).

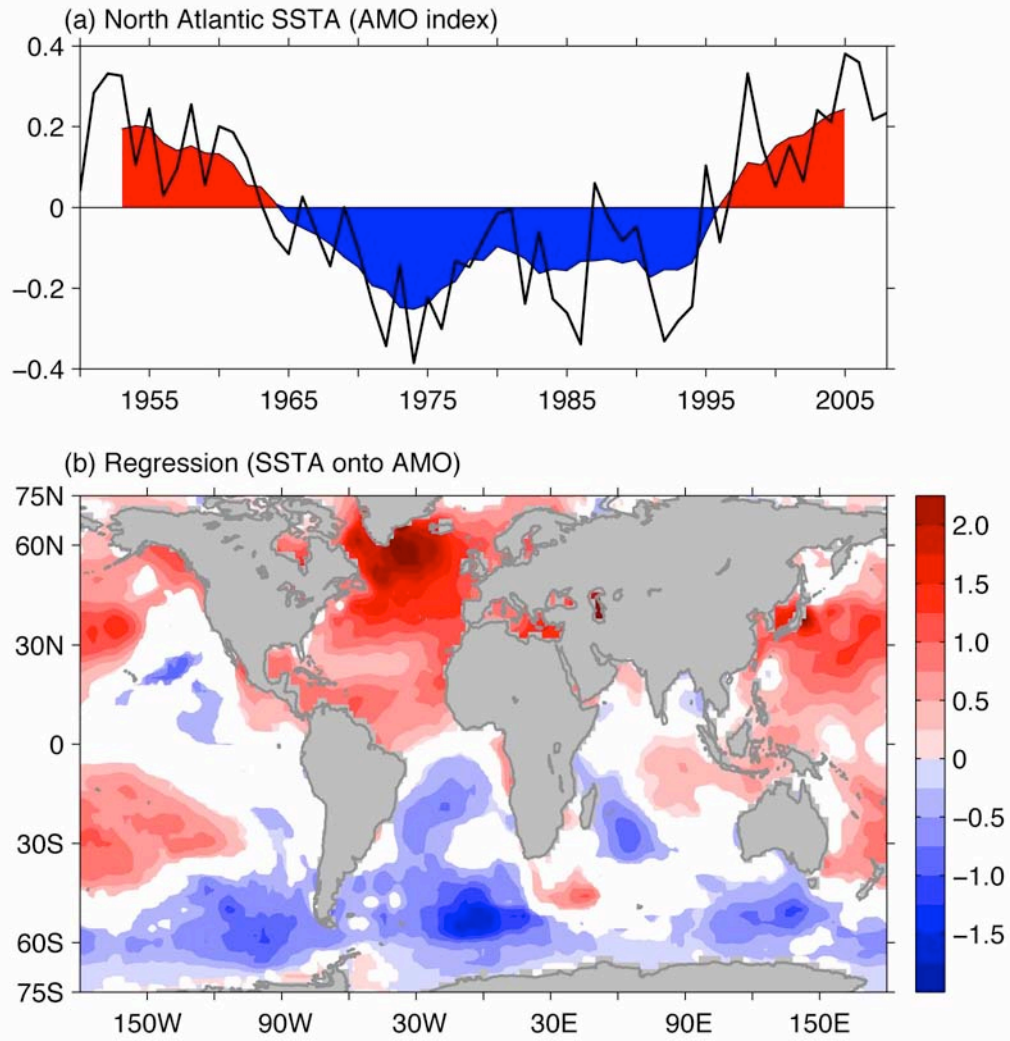


Figure 1. The AMO index and its relationship with global ocean SST. Shown are (a) the detrended annual SST anomalies (°C) in the North Atlantic of 0°-60°N and from the east coast of the Americas to 0° longitude and (b) regression (°C per °C) of global annual SST anomalies onto the AMO index. The regression is calculated based on the 7-year running mean data. The shading in (a) represents the 7-year running mean time series. The only regression exceeding the 95% significant level is plotted in (b).

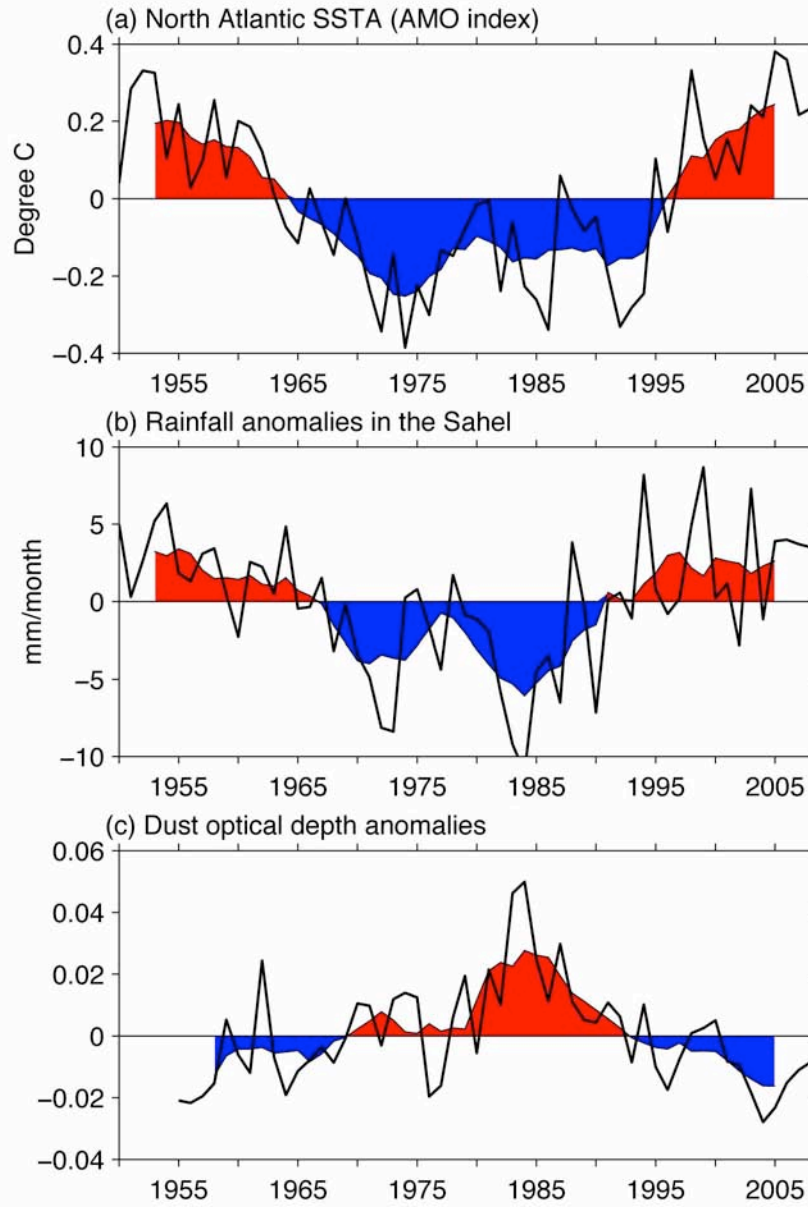


Figure 2. The AMO, Sahel rainfall and dust in the tropical North Atlantic. Shown are (a) the AMO index ($^{\circ}\text{C}$), (b) the annual rainfall anomalies (mm/month) in the Sahel (10°N - 20°N , 20°W - 40°E), and (c) the annual dust aerosol optical depth anomalies in the tropical North Atlantic (0° - 30°N , 10°W - 65°W). The shading represents the time series of 7-year running means.

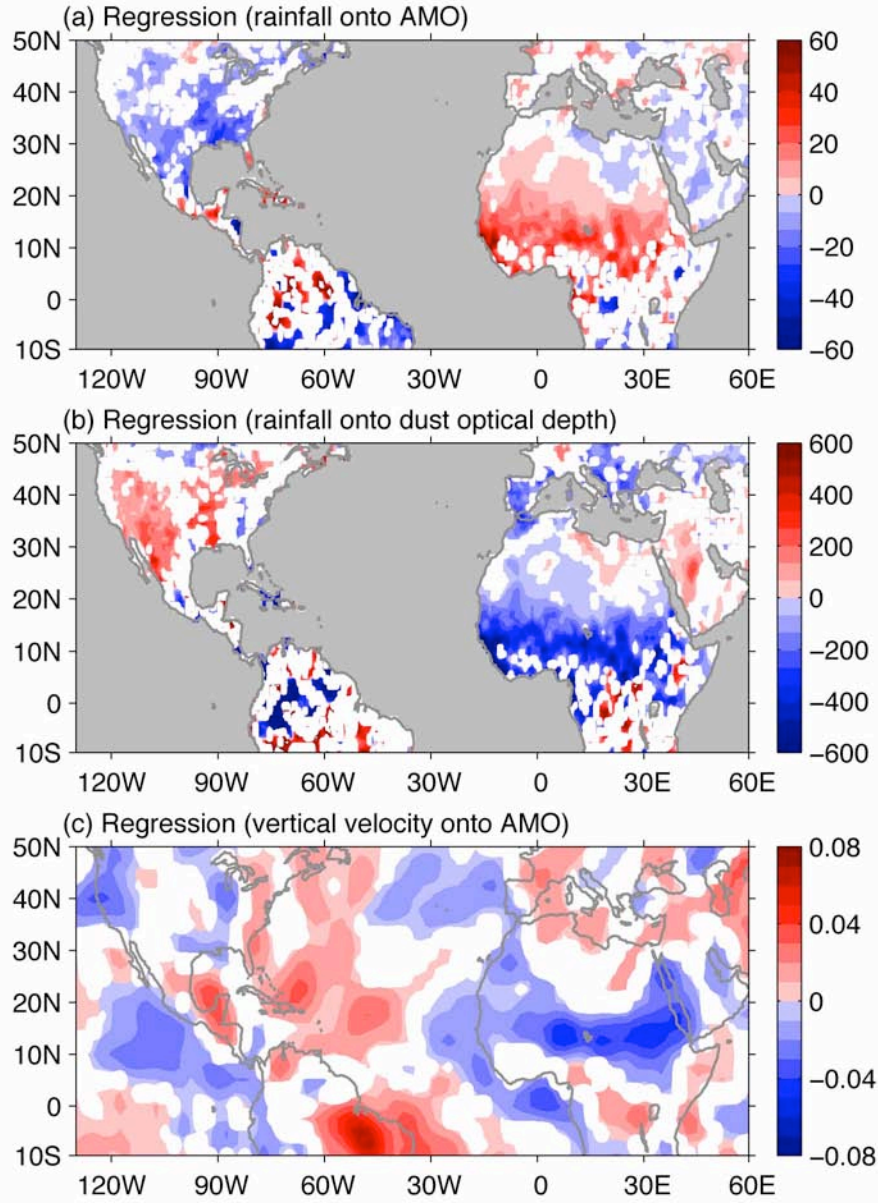


Figure 3. Linkage of the AMO, rainfall and aerosols. Shown are (a) regression (mm/month per $^{\circ}\text{C}$) of annual rainfall anomalies onto the AMO index, (b) regression (mm/month per DAOD) of annual rainfall anomalies onto the DAOD time series in the tropical North Atlantic, and (c) regression (Pa/s per $^{\circ}\text{C}$) of annual 500-hPa vertical pressure velocity anomalies onto the AMO index. The regressions are calculated based on the 7-year running mean data. The only regressions exceeding the 95% significant level are plotted.

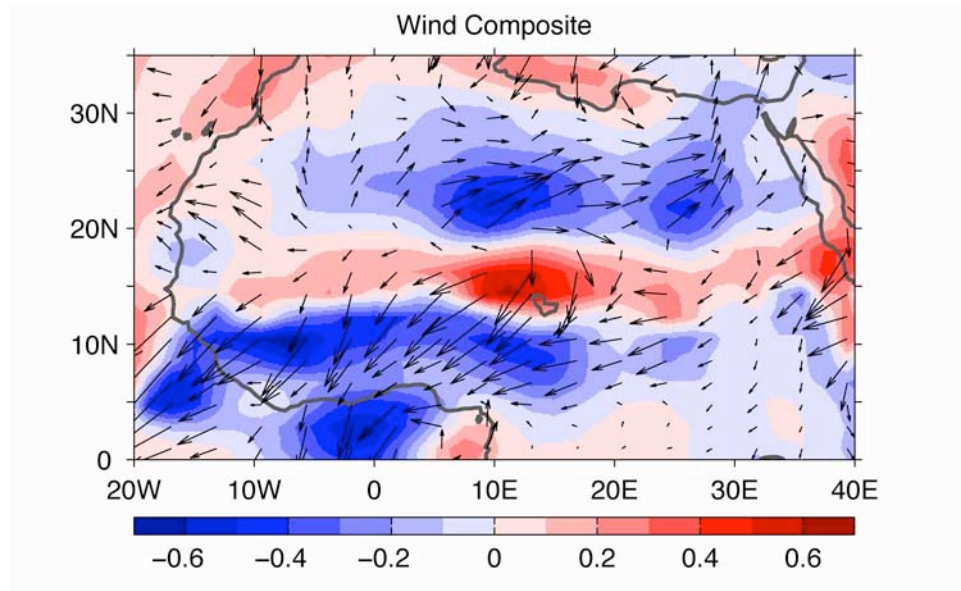


Figure 4. Relationship of surface wind with dust aerosol optical depth (DAOD) in the tropical North Atlantic. Shown is the 10-m wind composite difference between the highest and lowest DAOD years. The contoured shading represents the wind speed (m/s). The top and bottom quartiles of the DAOD time series are identified as the highest and lowest DAOD years, respectively.

Supplementary Information for

**Multidecadal Co-variability of North Atlantic Sea Surface Temperature,
African dust, and Sahel Rainfall**

Chunzai Wang¹

Shenfu Dong^{1 & 2}

Amato T. Evan³

Gregory R. Foltz¹

Sang-Ki Lee^{1 & 2}

¹ NOAA Atlantic Oceanographic and Meteorological Laboratory
Miami, Florida

² Cooperative Institute for Marine and Atmospheric Studies
University of Miami
Miami, Florida

³ Department of Environmental Sciences
University of Virginia
Charlottesville, Virginia

Submitted to *Nature* as a Letter

March 31, 2011

Supplementary Information

This supplementary information contains the description of data sets used in this study and five figures (Figs. S1-S5) referenced in the main text.

Data sets

Several data sets are used in this study. The first one is an improved extended reconstructed sea surface temperature (ERSST) data set on a 2° latitude by 2° longitude grid¹. The second data set is the National Centers for Environmental Prediction-National Center for Atmospheric Research (NCEP-NCAR) reanalysis on a 2.5° latitude by 2.5° longitude grid². Both of two data sets used here are monthly. Climatology is calculated based on the data from 1950 to 2008. Anomalies are then calculated by subtracting climatology from the monthly data.

The rainfall data set is from the Global Precipitation Climatology Centre (GPCC) Version 5. The monthly rainfall data is gridded from the complete GPCC station database with more than 70000 different raingauge stations worldwide³. The gridded land precipitation is available for the period 1901-2009 in spatial resolutions of $0.5^\circ \times 0.5^\circ$, $1.0^\circ \times 1.0^\circ$, and $2.5^\circ \times 2.5^\circ$. The data is available for downloading from ftp://ftp-anon.dwd.de/pub/data/gpcc/html/fulldata_download.html.

The extended dust aerosol optical depth (DAOD) over the tropical North Atlantic from 1955 to 2008 was derived from a simple model using modern and historical data from meteorological satellites and a proxy record for atmospheric dust⁴. Satellite data include aerosol optical thickness retrievals from the Advanced Very High Resolution Radiometer (AVHRR) Pathfinder Extended dataset (PATMOS-x) for the period 1982-2008 and the Moderate

Resolution Imaging Spectroradiometer (MODIS) on board the Aqua satellite for the period 2002–2008. The proxy record for atmospheric dust is based on measurements of crustal helium-4 (^4He) flux from a *Porites* coral at a water depth of 5 m near Pedra de Lume on Sal Island ($16^{\circ}45'44''$ N, $22^{\circ}53'23''$ W), part of the Cape Verde archipelago, for the period of 1955–94⁵. The resultant 54-yr record of DAOD has a $1.0^{\circ}\times 1.0^{\circ}$ spatial resolution and a monthly temporal resolution, and covers the region 0° – 30° N, 10° – 65° W.

Figures S1 to S5

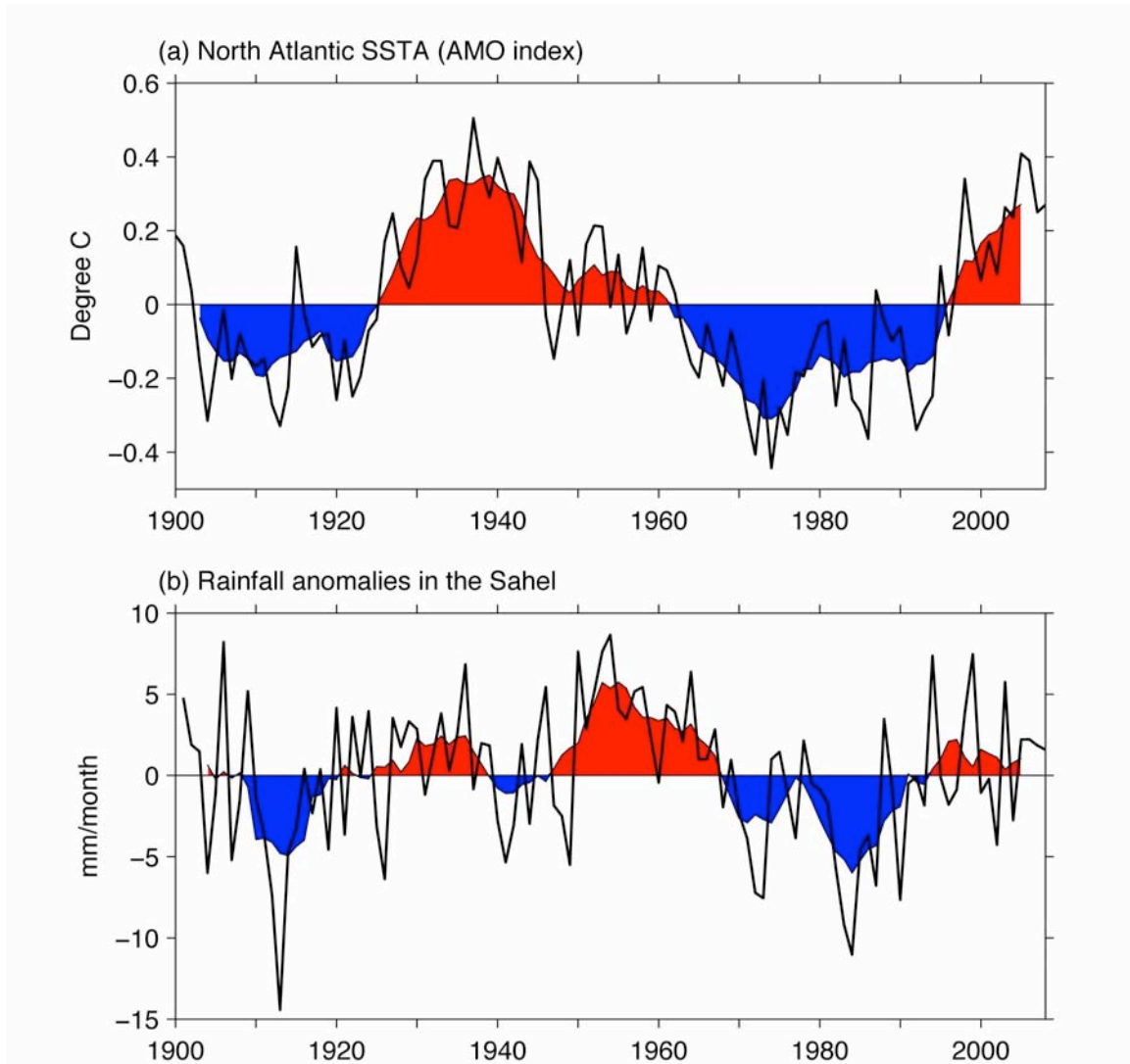


Figure S1. The AMO index and Sahel rainfall time series for a long-term record of 1900-2008. Shown are (a) the AMO index ($^{\circ}\text{C}$) and (b) the annual rainfall anomalies (mm/month) in the Sahel (10°N - 20°N , 20°W - 40°E). The time series are detrended and the shading represents the time series of 7-year running means.

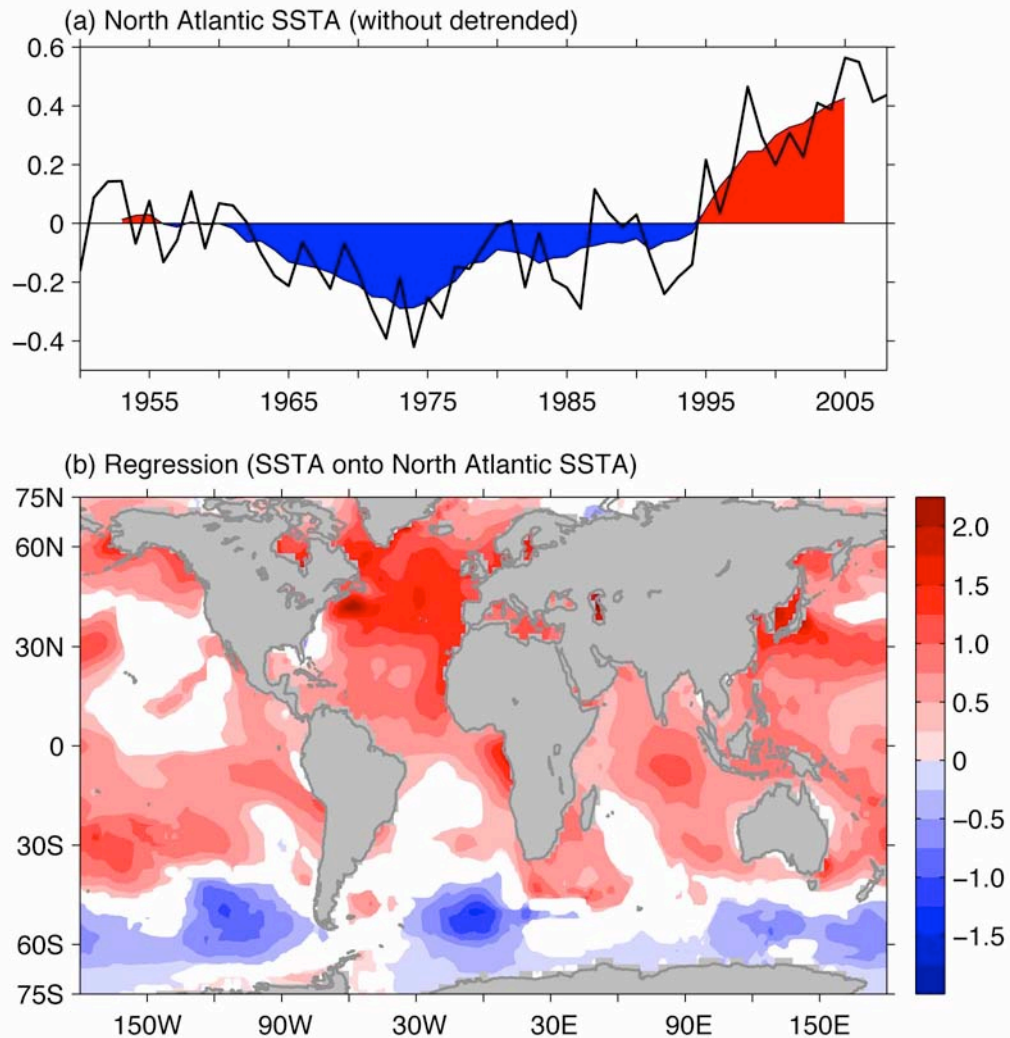


Figure S2. The time series of the North Atlantic SST anomalies and its regressed map using the data with the linear trends included. Shown are (a) the annual SST anomalies ($^{\circ}\text{C}$) in the North Atlantic of 0° - 60°N and from the east coast of the Americas to 0° longitude and (b) regression ($^{\circ}\text{C}$ per $^{\circ}\text{C}$) of global annual SST anomalies onto the North Atlantic SST index of (a). The regression is calculated based on the 7-year running mean data. The only regression exceeding the 95% significant level is plotted. The shading in (a) represents the time series of 7-year running means.

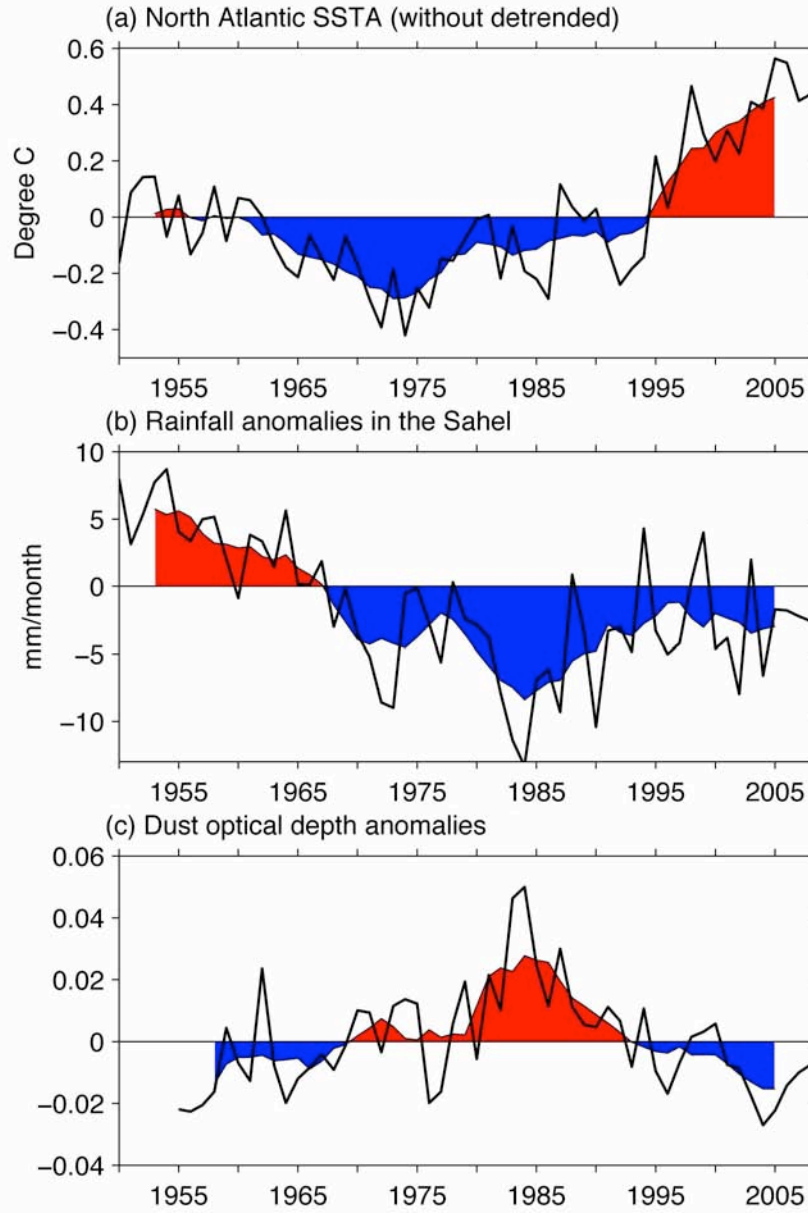


Figure S3. The time series of the North Atlantic SST, Sahel rainfall and dust in the tropical North Atlantic using the data with the linear trends included. Shown are (a) the annual SST anomalies ($^{\circ}\text{C}$) in the North Atlantic of 0° - 60°N and from the east coast of the Americas to 0° longitude, (b) the annual rainfall anomalies (mm/month) in the Sahel (10°N - 20°N , 20°W - 40°E), and (c) the annual dust aerosol optical depth (DAOD) anomalies in the tropical North Atlantic (0° - 30°N , 10°W - 65°W). The shading represents the time series of 7-year running means.

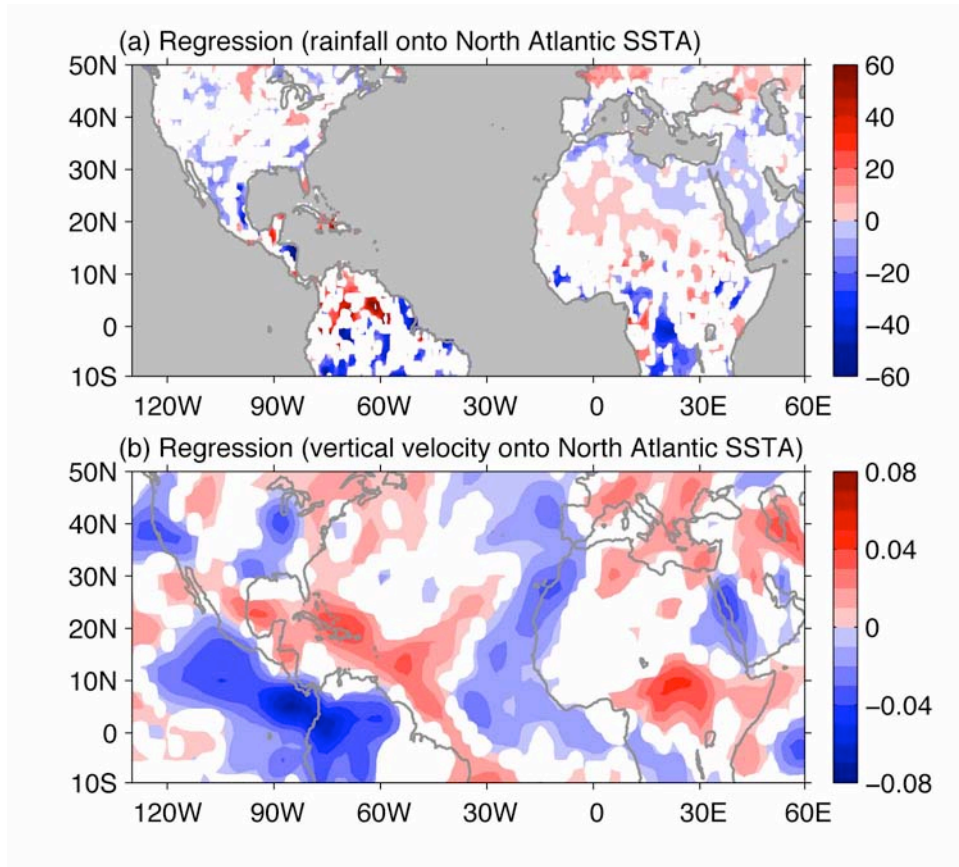


Figure S4. Linkage of the North Atlantic SST with rainfall using the data with the linear trends included. Shown are (a) regression (mm/month per °C) of annual rainfall anomalies onto the North Atlantic SST index and (b) regression (Pa/s per °C) of annual 500-hPa vertical pressure velocity anomalies onto the North Atlantic SST index. The regressions are calculated based on the 7-year running mean data. The only regression exceeding the 95% significant level is plotted.

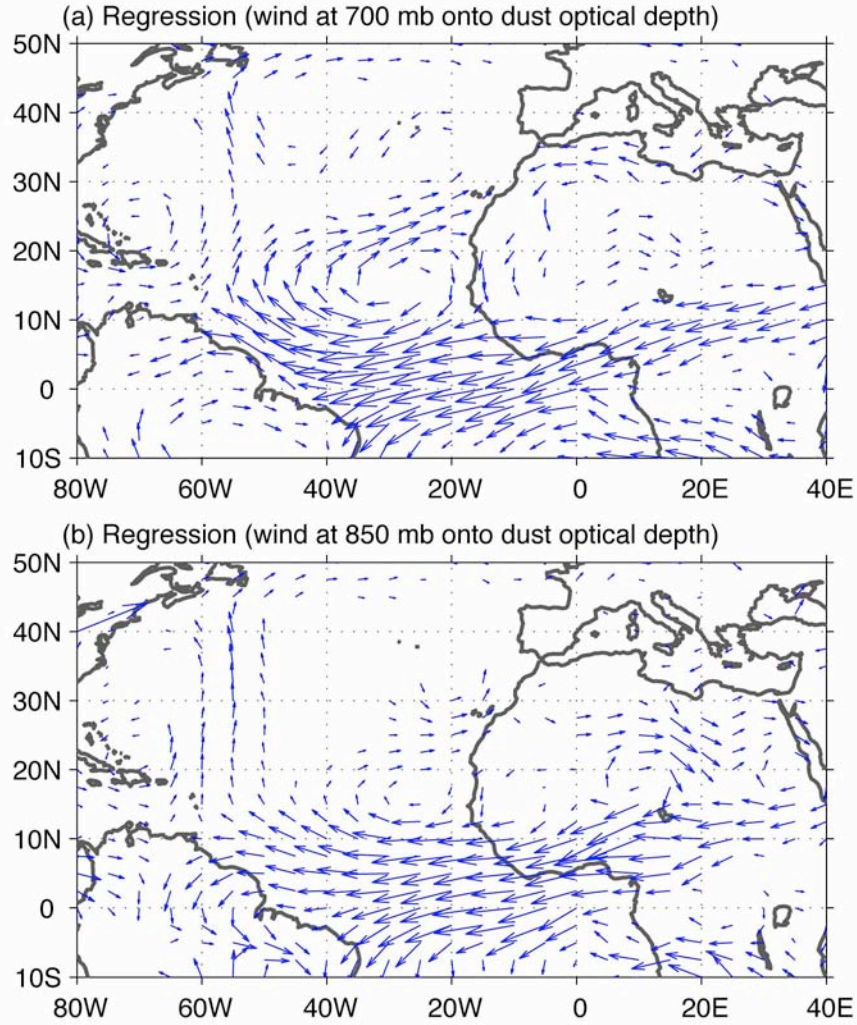


Figure S5. Winds associated with dust aerosol optical depth (DAOD) in the tropical North Atlantic. Shown are regressions (m/s per DAOD) of annual wind anomalies at (a) 700-hPa and (b) 850 hPa onto the DAOD time series. The regressions are calculated based on the detrended and 7-year running mean data. The only regressions exceeding the 95% significant level are plotted.

References

1. Smith, T. M., Reynolds, R.W., Peterson, T. C. & Lawrimore, J. Improvements to NOAA's historical merged land-ocean surface temperature analysis (1880-2006). *J Clim.* **21**, 2283-2296 (2008).
2. Kalnay, E. et al. The NCEP/NCAR 40-year reanalysis project. *Bull. Am. Meteorol. Soc.* **77**, 437-471 (1996).
3. Rudolf, B., Hauschild, H., Ruth, W. & Schneider, U. Terrestrial precipitation analysis: Operational method and required density of point measurements. *Global Precipitation and Climate Change*, M. Dubois and M. Desalmand, Eds., Springer-Verlag, 173–186 (1994).
4. Evan, A. T. & Mukhopadhyay, S. African Dust over the Northern Tropical Atlantic: 1955–2008. *J. Appl. Meteor. Climatol.*, **49**, 2213–2229 (2010).
5. Mukhopadhyay, S. & Kreycik, P. Dust generation and drought patterns in Africa from helium-4 in a modern Cape Verde coral. *Geophys. Res. Lett.* **35**, L20820, doi:10.1029/2008GL035722 (2008).